NANO LETTERS

LETTER

pubs.acs.org/NanoLett

Enhancing the Radiative Rate in III−V Semiconductor Plasmonic Core−Shell Nanowire Resonators

Carrie E. Hofmann,[†] F. Javier García de Abajo,[‡] and Harry A. Atwater*,[†]

[†]Thomas J. Watson Laboratory of Applied Physics, California Institute of Technology, Pasadena, California 91125, United States

[‡]Instituto de Óptica, CSIC, Serrano 121, 28006 Madrid, Spain

ABSTRACT: We investigate the radiative properties of plasmonic core−shell nanowire resonators and, using boundary element method calculations, demonstrate enhanced radiative decay rate by up to 3500 times in nanoscale compound semiconductor/metal cavities. Calculation of the local density of optical states enables identification of new types of modes in cavities with mode volumes on the order of $10^{-4}(\lambda/n)^3$. These modes dramatically enhance the radiative decay rate and significantly modify the polarization of far-field emission.

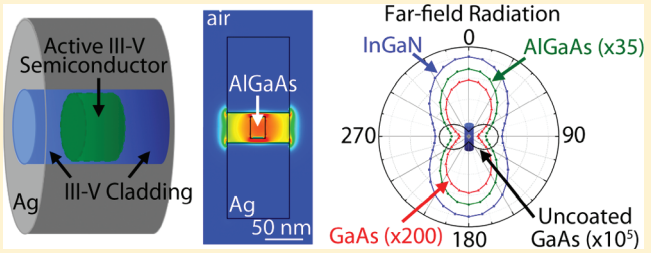

KEYWORDS: Plasmonic resonator, core−shell nanowire, radiative rate enhancement, local density of optical states, Purcell effect

In 1946, Purcell reported that the radiative decay rate could be modified when the emission is coupled to a resonant cavity,[1] and since then researchers have devoted considerable effort to enhancing light emission from semiconductors and molecules using optical geometries that exhibit high Purcell factors. To effectively enhance the rate of radiative emission, one must maximize the quantity of Q/V, where Q is the quality factor of the resonance and V is the modal volume. In conventional dielectric cavities, high Q/V factors are traditionally achieved by creating resonators with high quality factors ($Q > 10^6$), but in volumes larger than $(\lambda/n)^3$, where λ is the wavelength and n is the refractive index. In plasmonic cavities such as the core−shell nanowire resonators described here, modes with low quality factors ($Q < 50$) are confined to subwavelength effective mode volumes V_{eff} and thus can achieve high figures of merit Q/V_{eff}. It has long been recognized that metal films and nanostructures can enhance the fluorescence of molecules[2,3] and semiconductors,[4,5] and more recently a number of more complex plasmonic nanoparticle and nanoantenna geometries have been employed to modify the radiative emission rate.[6,7a,7b] Previous work demonstrated greater than 90 times[8] and greater than 40 times[5] plasmonic enhancement of radiative emission for InGaN quantum wells in planar and metal nanoparticle geometries. We have achieved a much more dramatic emission rate enhancement of greater than 3000 times by coupling directly to the active semiconductor region in a cylindrical geometry. Achieving high Purcell enhancements by confining the active region in a subwavelength cavity, one can access a regime in which spontaneous emission rates exceed stimulated emission rates, potentially enabling modulation speeds much faster than lasers.[9] In this Letter, we apply the so-called zero mode of a subwavelength hole[10] to a cylindrical plasmonic nanocavity[11,12] and demonstrate that this ultrasmall mode volume resonator dramatically enhances the radiative decay rate of active semiconductor materials.

We investigate plasmonic core−shell nanowire resonators consisting of a III−V compound semiconductor heterostructure nanowire core surrounded by an optically thick Ag coating, shown schematically in Figure 1a. Enhancing the spontaneous emission rate of III−V semiconductors is of particular interest because they have high internal quantum efficiency and an ability to form high-quality heterostructures. The semiconductor heterostructure core has an active light emitting region (length L_A, radius a) clad on all sides with a larger band gap material (length L_C and thin spacer layer thickness s), an Ag coating thickness T, and a total resonator length $L = L_A + 2L_C$. This geometry allows for significant modification of the local density of optical states (LDOS), which describes the available optical eigenmodes for photons at a specific position, orientation, and frequency. The decay rate of excited atoms is proportional to the LDOS. Changing the material and dimensions of the semiconductor core directly modifies the LDOS and thus controls the total and radiative decay rates. Furthermore, we take advantage of the modest quality factors in these plasmonic nanostructures ($Q < 50$) to achieve band-to-band decay rate enhancement. We use the boundary element method (BEM) to investigate the LDOS in these structures,[13,14] choosing dimensions of the resonator such that the lowest order longitudinal mode overlaps with the emission wavelength of the active material. For this mode, we determine the LDOS, effective mode volume (V_{eff}), quality factor (Q), enhancements in the total and radiative decay rates (Γ_{tot} and Γ_{rad}, respectively, normalized to decay in vacuum, Γ_0), and the corresponding quantum efficiency, $\eta = \Gamma_{rad}/\Gamma_{tot}$.

In the BEM, calculations are performed in the frequency domain with the electromagnetic field in each homogeneous

Received: August 13, 2010
Revised: October 20, 2010
Published: January 18, 2011

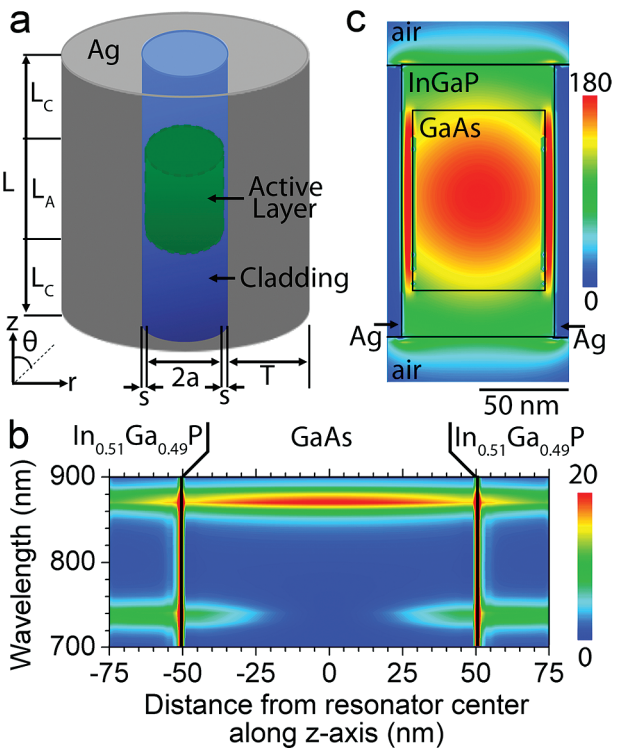

Figure 1. (a) Schematic of a plasmonic core−shell nanoresonator. The nanowire core consists of a III−V semiconductor active layer (length L_A and radius a) clad with a wider band gap III−V semiconductor (segment lengths L_C and spacer thickness s) and coated with Ag (thickness T and total length $L = 2L_C + L_A$). (b) Resonant modes for a structure with GaAs active layer (a = 36 nm, L_A = 100 nm), $In_{0.51}Ga_{0.49}P$ cladding (s = 5 nm, L_C = 25 nm), and Ag coating thickness T = 100 nm. The LDOS is calculated at a constant radial position of r = 1 nm from the center of the resonator core and normalized to the LDOS in vacuum. (c) Two-dimensional NF $|\mathbf{E}|^2$ cross section for plane-wave excitation at λ = 870 nm (θ = 0°), the emission wavelength of GaAs.

region expressed as a function of auxiliary boundary charges and currents. After boundary conditions are applied, a set of linear integrals is obtained and solved by discretization. The axial symmetry of core−shell nanowire resonators allows decomposition of the fields into uncoupled azimuthal components m with angular dependence $e^{im\phi}$. This results in an essentially one-dimensional field calculation that is solved with great accuracy. Converged results are found for values of m defined by $m = -1$, 0, 1, and the lowest order $\lambda/2$ mode we investigate here has m = 1 symmetry.

The dielectric functions of the core and cladding materials are input using tabulated data.[15−19] The frequencies ω of the relevant resonant modes that produce enhanced emission are determined by calculating the LDOS ρ for a dipole emitter oriented along a radial direction using the relation[20]

$$\rho = \frac{\omega^2 n}{3\pi^2 c^3} + \frac{1}{2\pi^2 \omega}\,\mathrm{Im}\{E_{\mathrm{scat}}/D\} \qquad (1)$$

where c is the speed of light in vacuum, n is the refractive index of the active semiconductor, D is the dipole strength, and E_{scat} is the contribution to the electric field due to scattering at the interfaces, evaluated at the position of the emitter, and projected along the direction of polarization. The resonance quality factor, Q, is determined by fitting a Lorentzian line shape to a plot of ρ vs ω, and $Q = \omega/\Delta\omega$, where $\Delta\omega$ is the full width at half-maximum.

Besides calculating the LDOS, we determine the spatial near-field electric field intensity (NF $|\mathbf{E}|^2$) profiles of each mode by using plane-wave excitation incident at $\theta = 0°$, polarized along an arbitrary radial direction (see Figure 1a). The effective mode volume V_{eff} is defined as a cylinder with length L_{eff} and radius a_{eff} given by the $1/e$ decay distance of the peak field intensity inside the semiconductor core, such that $V_{\mathrm{eff}} = \pi a_{\mathrm{eff}}^2 L_{\mathrm{eff}}$. To determine what portion of the decay contributes to radiative emission and absorption, we assume that the compound semiconductor active material has unit internal quantum efficiency in homogeneous bulk materials[21] and for dipoles located inside the active region calculate the enhancements in the total and radiative decay rates normalized to Γ_0, the decay rate in vacuum, given by

$$\Gamma_0 = \frac{4}{3}\frac{|D_{\mathrm{vac}}|^2}{\hbar}\left(\frac{\omega}{c}\right)^3 \qquad (2)$$

where D_{vac} is the dipole strength in vacuum. The total decay rate, Γ_{tot}, is related to the LDOS ρ as

$$\Gamma_{\mathrm{tot}} = \frac{4\pi^2\omega|D|^2}{\hbar}\rho \qquad (3)$$

where the relation $D = (3n^2/(2n^2 + 1))^* D_{\mathrm{vac}}$ originates in local-field corrections for emission inside a dielectric of refractive index n.

Finally, the radiative decay rate, Γ_{rad}, is calculated by integrating the far-field Poynting vector for a dipole source (polarized along r) located in the center of the resonator core. If instead of considering an arbitrary radial direction, we perform an isotropic average of the radial (x and y) and longitudinal (z) dipoles in both Γ_{tot} and Γ_{rad} calculations, the values we report for the total and radiative decay rates are decreased by approximately 33%, as the longitudinal dipole does not couple efficiently to the desired mode.

Detailed results are presented for three resonators, each composed of a different III−V compound semiconductor active emitter (GaAs, $Al_{0.42}Ga_{0.58}As$, and $In_{0.15}Ga_{0.85}N$). We first consider GaAs as an active material with a band gap (emission wavelength) E_g = 1.424 eV (λ = 870 nm), clad with $In_{0.51}Ga_{0.49}P$. A thin $In_{0.51}Ga_{0.49}P$ spacer layer is located between the GaAs active region and Ag coating to prevent quenching of excitons located near the metal/semiconductor interface. The lowest-order longitudinal mode occurs at the proper wavelength for a resonator with dimensions a = 36 nm, s = 6 nm, L_A = 100 nm, L_C = 25 nm, and T = 100 nm. Figure 1b is a contour plot of the LDOS as a function of both wavelength and distance along the z axis at a constant radial position of r = 1 nm. We evaluate the LDOS at a distance of 1 nm from the axis of the structure in order to avoid pathological divergences arising when evaluating gradients and rotationals in cylindrical coordinates. Nevetheless, the variation of the LDOS over such small radial distance is negligible. It is clear from this plot that the mode at λ = 870 nm has LDOS peaked in the GaAs region of the core. Additional modes are supported at shorter wavelengths, but these do not overlap with the emission wavelength of the active material and do not have the proper symmetry to support large decay rate enhancements. Plane wave excitation at λ = 870 nm allows investigation of the electric field localization, and high confinement of the fields in both the radial and longitudinal directions is demonstrated in the two-dimensional NF $|\mathbf{E}|^2$ cross section of Figure 1c. The regions of high field intensity in the core correlate to regions of high LDOS and thus also to large enhancements in the total decay rate. This mode has a moderate quality factor of

dx.doi.org/10.1021/nl102878b |Nano Lett. 2011, 11, 372–376

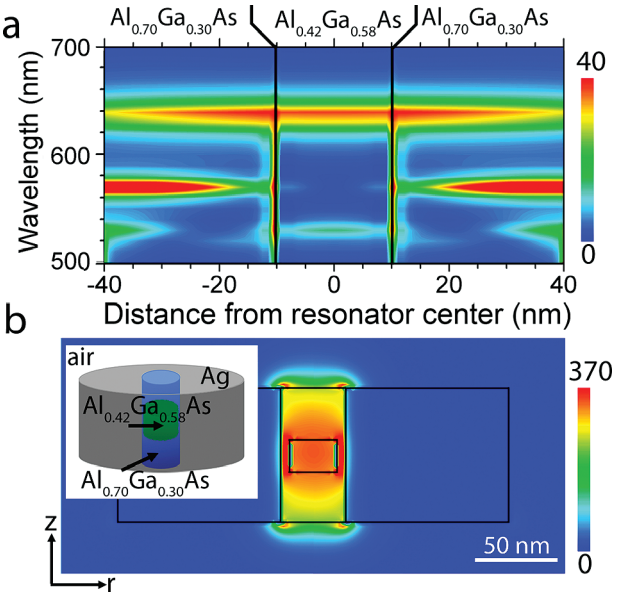

Figure 2. (a) LDOS showing the resonant modes for a structure with $Al_{0.42}Ga_{0.58}As$ active layer (a = 15 nm, L_A = 20 nm), $Al_{0.70}Ga_{0.30}As$ cladding (s = 5 nm, L_C = 30 nm), and Ag coating (T = 100 nm), calculated at a constant radial position of r = 1 nm from the center of the resonator core and normalized to the LDOS in vacuum. (b) Two-dimensional NF $|\mathbf{E}|^2$ cross section for the resonance at the $Al_{0.42}Ga_{0.58}As$ emission wavelength of λ = 637 nm (plane wave excitation at $\theta = 0°$).

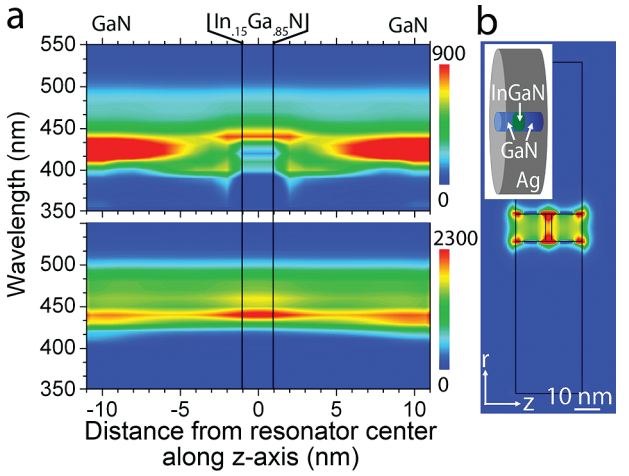

Figure 3. (a) LDOS (normalized to LDOS in vacuum) and NF $|\mathbf{E}|^2$ vs wavelength and (b) cross-sectional NF $|\mathbf{E}|^2$ profile for a structure with $In_{0.15}Ga_{0.85}N$ active layer (a = 5 nm, L_A = 2 nm), GaN cladding (L_C = 10 nm and no spacer layer), and Ag coating (T = 50 nm). LDOS and NF $|\mathbf{E}|^2$ in (a) are calculated at a radial position of r = 1 nm from the center. Two-dimensonal NF $|\mathbf{E}|^2$ is calculated for plane-wave excitation at λ = 440 nm ($\theta = 0°$), the emission wavelength of the InGaN quantum well.

45 and $V_{eff} = 0.070(\lambda/n)^3$, for $Q/V_{eff} = 645(\lambda/n)^{-3}$. The decay rate enhancements are calculated for a dipole located in the center of the resonator polarized along the r direction, and we find $\Gamma_{tot}/\Gamma_0 = 223$, $\Gamma_{rad}/\Gamma_0 = 128$, and $\eta = 0.57$.

To investigate smaller structures with modes at shorter wavelengths, we chose $Al_{0.42}Ga_{0.58}As$ as the active material. This alloy has E_g = 1.95 eV, emitting at a wavelength of λ = 637 nm. A ternary alloy with higher Al content, $Al_{0.70}Ga_{0.30}As$, is chosen for the cladding and spacer material, which is an indirect band gap semiconductor with E_g = 2.07 eV. A core−shell nanowire resonator composed of these materials with dimensions a = 14 nm, s = 5 nm, L_A = 20 nm, L_C = 30 nm, and T = 100 nm has the lowest order longitudinal mode at λ = 637 nm. The LDOS mode profile along the length of the resonator, calculated at a radial position of r = 1 nm from the center of the core, is shown in Figure 2a. Note the 2-fold increase in LDOS of the lowest order mode as compared to the larger GaAs structure. The two-dimensional NF $|\mathbf{E}|^2$ profile for the mode at λ = 637 nm in Figure 2b demonstrates that even in this smaller structure, fields are highly confined in the semiconductor core with minimal field penetration into the surrounding medium. This mode has Q = 30, $V_{eff} = 0.021(\lambda/n)^3$, and $Q/V_{eff} = 1435(\lambda/n)^{-3}$, with decay rate enhancement $\Gamma_{tot}/\Gamma_0 = 460$, $\Gamma_{rad}/\Gamma_0 = 280$, and $\eta = 0.60$. Comparing these results to the GaAs resonator, we see that the smaller resonator continues to exhibit high modal confinement with a V_{eff} approximately equal to the physical volume of the semiconductor core and that the lowest-order mode does not sustain much loss in quality factor with decreased dimensions. Thus, the figure of merit Q/V_{eff} more than doubles in this smaller resonator relative to the first example using GaAs, described above.

Next, we consider as our active layer a 2 nm $In_{0.15}Ga_{0.85}N$ single quantum well (SQW), with GaN as the cladding. Excitons in the $In_{0.15}Ga_{0.85}N$ are highly localized, and therefore an explicit spacer layer is not modeled in this structure. The $In_{0.15}Ga_{0.85}N$ quantum well emits at λ = 440 nm, and the resonator with the lowest-order longitudinal mode at this wavelength has dimensions of a = 5 nm, L_A = 2 nm, L_C = 10 nm, and T = 50 nm. In this deeply subwavelength resonator, only extremely evanescent modes are supported. The LDOS and NF $|\mathbf{E}|^2$ for plane-wave excitation at $\theta = 0°$ along the length of the wire are shown in Figure 3a. At λ = 440 nm, the peak LDOS is localized within the $In_{0.15}Ga_{0.85}N$ SQW with a peak value of 900, more than 20 times the peak LDOS of the GaAs and $Al_{0.42}Ga_{0.58}As$ resonators. Additionally, the NF $|\mathbf{E}|^2$ cross section in Figure 3b illustrates the high level of confinement within the core of this deeply subwavelength structure and a peak electric field intensity of 3000 times larger than the incident plane wave. This highest LDOS and NF $|\mathbf{E}|^2$ of the three resonators studied in detail here is achieved with the smallest resonator volume. We calculate Q = 32 and $V_{eff} = 4.3 \times 10^{-4}(\lambda/n)^3$ and find the highest Q/V_{eff} in this ultrasmall resonator at $7.4 \times 10^4(\lambda/n)^{-3}$. Dramatic decay rate enhancements are found for this structure, with $\Gamma_{tot}/\Gamma_0 = 8200$, $\Gamma_{rad}/\Gamma_0 = 3500$, and $\eta = 0.43$, which exceeds the radiative decay rate enhancements reported for metal nanoparticle structures by more than 30 times.[8] This demonstrates that upon the transition from subwavelength resonators that support eigenmodes with sizable retardation effects to ultrasmall resonators that support highly evanescent modes of nonretarded nature, plasmonic core−shell nanowire resonators with dimensions on the order of $\lambda/50$ are able to strongly confine modes within the semiconductor core and to achieve dramatic enhancements in the radiative decay rate.

The total decay rate enhancements and corresponding quantum efficiencies are plotted in Figure 4. Peaks in the plot of Γ_{tot}/Γ_0 versus wavelength correspond to the resonant modes illustrated in the LDOS plots of Figure 1b, Figure 2a, and Figure 3a. The largest decay rate enhancements are seen for the λ = 440 nm mode of the ultrasmall $In_{0.15}Ga_{0.85}N$ resonator, although significant enhancements are also observed for the GaAs and $Al_{0.42}Ga_{0.58}As$ resonators. Additionally, the quantum efficiencies

dx.doi.org/10.1021/nl102878b |*Nano Lett.* 2011, 11, 372–376

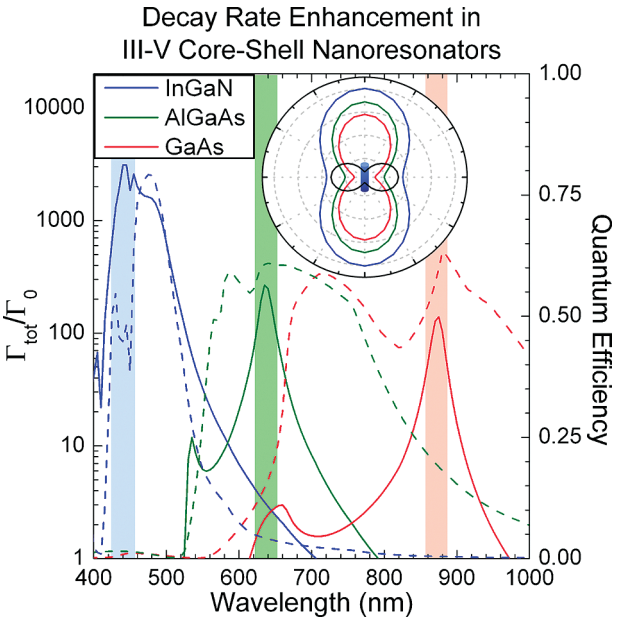

Figure 4. Total decay rate enhancement (solid) and quantum efficiencies (dashed) as a function of wavelength for the three different III−V core−shell nanoresonators. Colored shaded regions indicate typical spectral width of LED emission. (inset) Polar plot of far-field radiation from dipole excitation of the same three core−shell nanoresonators (AlGaAs scaled ×35, GaAs scaled ×200) and in black a bare (uncoated, no Ag) GaAs/$In_{0.51}Ga_{0.49}P$ nanowire (scaled ×10^5). The Ag coating modifies both the intensity and direction of the far-field emission.

η at the wavelengths of interest are >50% for these two resonators. Remarkably, even the smallest resonator ($In_{0.15}Ga_{0.85}N$ SQW) maintains a reasonable quantum efficiency >40%, suggesting that a large portion of the enhanced total decay rate correlates to observable photons. The colored shaded regions on the graph correspond to a typical LED bandwidth centered at the emission wavelength of the active material, and because of the moderate quality factors in these plasmonic resonators, the decay rates are enhanced significantly throughout the entire band.

Finally, we also calculate the polarization dependence of the far-field radiation at the emission wavelength of each III−V semiconductor plasmonic core−shell nanowire resonators and compare that to the emission polarization from an uncoated wire (GaAs active region with a = 36 nm, L_A = 100 nm, $In_{0.51}Ga_{0.49}P$ cladding and spacer with s = 6 nm and L_C = 25 nm, and no Ag coating). The polar plot is seen in the inset of Figure 4 for an observer looking down a radial axis. The far-field radiation is determined for dipole excitation in the center of the resonator core, and the emission is isotropically averaged for all three dipole orientations (x, y, and z). The uncoated wire has a dipolar emission pattern oriented transverse to the longitudinal axis of the nanowire. Although not plotted here, the uncoated wires with $In_{0.15}Ga_{0.85}N$ and $Al_{0.42}Ga_{0.58}As$ active regions show the same dipolar radiation pattern. With the Ag coating, all three of the resonators have a strongly modified emission polarization that is now oriented parallel to the longitudinal axis of the resonator. Thus, the plasmonic coating modifies not only the total and radiative decay rates but also the direction of far-field radiation. The detailed geometry of the coating controls the emission direction, as observed in the decay of single molecules placed close to a nanoantenna.[22]

Table 1. Summary of Q/V and Decay Rate Enhancements in III−V Semiconductor Plasmonic Core−Shell Nanowire Resonators

active material	GaAs	$Al_{0.42}Ga_{0.58}As$	$In_{0.15}Ga_{0.85}N$
radius a (nm)	36	14	5
length L_A (nm)	100 (GaAs)	20 ($Al_{0.42}Ga_{0.58}As$)	2 ($In_{0.15}Ga_{0.85}N$)
length L_C (nm)	25($In_{0.51}Ga_{0.49}P$)	30 ($Al_{0.70}Ga_{0.30}As$)	10 (GaN)
spacer s (nm)	6 ($In_{0.51}Ga_{0.49}P$)	4 ($Al_{0.70}Ga_{0.30}As$)	0
Ag thickness T (nm)	100	100	50
λ (nm)	870	637	440
V_{eff}	$0.070(\lambda/n)^3$	$0.021(\lambda/n)^3$	$4.3 \times 10^{-4}(\lambda/n)^3$
Q	45	30	32
Q/V_{eff}	$645(\lambda/n)^{-3}$	$1435(\lambda/n)^{-3}$	$74000(\lambda/n)^{-3}$
Γ_{rad}/Γ_0	128	280	3500
Γ_{tot}/Γ_0	223	460	8200
η (%)	57	60	43

In summary, we have introduced the III−V semiconductor plasmonic core−shell nanowire resonator geometry and shown that it is suitable for achieving dramatic decay rate enhancements for a variety of III−V materials, namely, GaAs, $Al_{0.42}Ga_{0.58}As$ and $In_{0.15}Ga_{0.85}N$. In all three structures, the dimensions are chosen such that the lowest-order longitudinal mode occurs at the band-edge emission wavelength of the active material, and the electric fields are highly confined within the resonator core. The increased LDOS due to the plasmonic coating contributes directly to enhanced emission, and total decay rate enhancements of >8000 with quantum efficiency of >40% are observed for a structure with dimensions on the order of $\lambda/50$. Additionally, $Q/V > 10^4(\lambda/n)^{-3}$ was calculated, a value competitive with conventional high-Q dielectric microcavities. The numerical results are summarized in Table 1. We anticipate that as we continue to shrink resonator dimensions and incorporate new active materials that emit near the surface plasmon resonance, even higher LDOS and radiative decay rate enhancements will be achievable. This work demonstrates that III−V semiconductor plasmonic core−shell nanoresonators are a promising design for fast, bright, nanoscale, and perhaps even directional on-chip light sources.

AUTHOR INFORMATION

Corresponding Author
*E-mail: haa@caltech.edu.

ACKNOWLEDGMENT

The authors acknowledge K. Aydin, R. Briggs, A. Hiszpanski, D. O'Carroll, and I. Pryce for insightful discussions and financial support from the Air Force Office of Scientific Research under Grant FA9550-09-1-0673. C.E.H. acknowledges fellowship support from the NSF and DOD.

REFERENCES

(1) Purcell, E. M. *Phys. Rev.* **1946**, *69*, 681.
(2) Drexhage, K. H. In *Progress in Optics XII*; Wolf, E., Ed.; North-Holland: Amsterdam, 1974; p 165.
(3) Gersten, J. I.; Nitzan, A. *Surf. Sci.* **1985**, *158*, 165.
(4) Vuckovic, J.; Loncar, M.; Scherer, A. *IEEE J. Quantum Electron.* **2000**, *36*, 1131.

(5) Okamoto, K.; Niki, I.; Shvarster, A.; Narukawa, Y.; Mukai, T.; Scherer, A. *Nat. Mater.* **2004**, *3*, 601.
(6) Tam, F.; Goodrich, G. P.; Johnson, B. R.; Halas, N. J. *Nano Lett.* **2007**, *7*, 496.
(7) (a) Kuhn, S.; Hakanson, U.; Rogobete, L.; Sandoghdar, V. *Phys. Rev. Lett.* **2006**, *97*, No. 017402. (b) Kuttge, M.; Garcia de Abajo, F. J.; Polman, A. *Nano Lett.* **2010**, *10*, 1537.
(8) Neogi, A.; Lee, C. W.; Everitt, H. O.; Kuroda, T.; Tackeuchi, A.; Yablonovitch, E. *Phys. Rev. B* **2002**, *66*, No. 153305.
(9) Lau, E. K.; Lakhani, A.; Tucker, R. S.; Wu, M. C. *Opt. Express* **2009**, *17*, 7790.
(10) Levene, M. J.; Korlach, J.; Turner, S. W.; Foquet, M.; Craighead, H. G.; Webb, W. W. *Science* **2003**, *299*, 682.
(11) Hill, M. T.; Oei, Y.-S.; Smallbrugge, B.; Zhu, Y.; de Vries, T.; van Veldhoven, P. J.; van Otten, F. W. M.; Eijkemans, T. J.; Turkiewicz, J. P.; de Waardt, H.; Geluk, E. J.; Kwon, S.-H.; Lee, Y.-H.; Notzel, R.; Smit, M. K. *Nat. Photonics* **2007**, *1*, 589.
(12) Nezhad, M. P.; Simic, A.; Bondarenko, O.; Slutsky, B.; Mizrahi, A.; Feng, L.; Lomakin, V.; Fainman, Y. *Nat. Photonics* **2010**, *4*, 395.
(13) García de Abajo, F. J.; Howie, A. *Phys. Rev. B* **2002**, *65*, No. 115418.
(14) Blanco, L. A.; García de Abajo, F. J. *Phys. Rev. B* **2004**, *69*, No. 205414.
(15) Johnson, P. B.; Christy, R. W. *Phys. Rev. B* **1972**, *6*, 4370.
(16) Aspnes, D. E.; Studna, A. A. *Phys. Rev. B* **1983**, *27*, 985.
(17) Schubert, M.; Gottschalch, V.; Herzinger, C. M.; Yao, H.; Snyder, P. G.; Woollam, J. A. *J. Appl. Phys.* **1995**, *77*, 3416.
(18) Tanguy, C. *Phys. Rev. Lett.* **1995**, *75*, 4090.
(19) Leung, M. M. Y.; Djurisic, A. B.; Li, E. H. *J. Appl. Phys.* **1988**, *84*, 6312.
(20) There is some ambiguity in the definition of the LDOS in dissipative media, and therefore, we have chosen to calculate it from the total decay rate as in eq 3. See ref 14 for further details of the derivation of eq 1.
(21) Anger, P.; Bharadwaj, P.; Novotny, L. *Phys. Rev. Lett.* **2006**, *96*, No. 113002.
(22) Taminiau, T. H.; Stefani, F. D.; Segerink, F. B.; van Hulst, N. F. *Nat. Photonics* **2008**, *2*, 234.